Kinetic and Equilibrium Studies of Porphyrin Interactions with Unilamellar Lipidic Vesicles†

Katerina Kuzelová and Daniel Brault*

Laboratoire de Biophysique, Inserm U.201, CNRS U.A. 481, Muséum National d'Histoire Naturelle, 43 rue Cuvier, 75231 Paris Cedex 05, France

Received December 28, 1993; Revised Manuscript Received June 8, 1994®

ABSTRACT: The interaction of deuteroporphyrin with dimyristoylphosphatidylcholine unilamellar vesicles of various sizes (ranging from 38 to 222 nm) has been studied using a stopped flow with fluorescence detection. Beside the kinetics of porphyrin incorporation into vesicles, the transfer of porphyrin from vesicles to human serum albumin has been investigated both experimentally and theoretically. The effects of both vesicle and albumin concentrations indicate that the transfer proceeds through the aqueous phase. It is governed by the rate of incorporation of porphyrin into the outer vesicle hemileaflet (k_{on}), by the exit to the bulk aqueous medium (k_{off}), and by the association (k_{as}) and dissociation (k_{dis}) constants relative to albumin. In both systems studied, a slower transbilayer flip-flop accounts for the biphasic character of the kinetics. This model is strongly supported by the effects of vesicle size, temperature, and cholesterol. The dependence of k_{on} on the vesicle size indicates that the incorporation is diffusion controlled. The constant k_{off} is found to be closely coupled to the phase state of the bilayer. The transbilayer flip-flop rate constant is approximately the same in both directions ($\sim$0.4 s^{-1} at 32 °C and pH 7.4). It is strongly affected by the presence of cholesterol in vesicles and by the temperature, with a sharp enhancement around the phase transition. With the exception of very small vesicles obtained by sonication, no influence of the vesicle size on the flip-flop rate was observed. An accelerating effect of tetrahydrofuran, used to improve the solubility of porphyrin, has been noted. Steady-state measurements and kinetics results were in excellent agreement. The interest of systems involving albumin as a scavenger to extract important rate constants, is emphasized.

New forms of selective therapies are being developed that are based on the generation of very toxic short-lived species upon the absorption of light by photosensitizing agents (Spikes & Straight, 1990). In a biological environment, these species, such as singlet oxygen, diffuse less than 0.1 μm (Moan & Berg, 1991) during their lifetime. Damages to biomolecules are thus determined by the localization of the photosensitizer. The charge and the hydrophobicity are the main determinants of subcellular localization of the photosensitizer (Berg et al., 1990; Oenbrink et al., 1988) and, consequently, of photobiological effects. Membrane structures, in particular mitochondria (Salet & Moreno, 1990), have been found to be particularly sensitive to photosensitization. A major application of photosensitization is the therapy of tumors which have been found to accumulate certain photosensitizers, in particular porphyrins, with some selectivity [for general reviews, see Dougherty et al. (1990) and Moan and Berg (1992)]. There is however considerable controversy concerning the mechanisms responsible for tumor selectivity and the nature of the main targets at cellular or tumor levels (Henderson & Dougherty, 1992).

A low-density lipoprotein receptor-mediated pathway, favored in tumor cells, has been suggested to be preponderant in the case of hydrophobic photosensitizers (Jori et al., 1984; Reyftmann et al., 1984; De Smidt et al., 1993). However, the correlation between the tumor selectivity and the affinity for low-density lipoproteins has been reported to be quite poor (Kongshaug et al., 1989). Alternatively, the low pH value of the interstitial fluid in tumors has been suggested to favor passive cellular incorporation of carboxylic porphyrins (Moan et al., 1980). This hypothesis gained support from studies on the interactions of porphyrins with membrane models (Brault et al., 1986) and from recent in vivo experiments (Thomas & Girotti, 1989; Peng et al., 1991). Note that in vitro studies have shown that the translocation of porphyrins within cells is quite fast (Shulock et al., 1990). Thus, it appears important to consider processes from a dynamic point of view whatever mechanisms are involved. Of particular importance is to know how photosensitizers can enter and cross bilayer structures such as the plasmic membrane, the lysosomal barrier, or the mitochondrial membranes and what are the determinants of these processes.

These questions have obvious relevance to the dynamics of various amphiphilic biomolecules (Zana, 1986) and have been considered in the cases of the fatty acid transport (Doody et al., 1980; Storch & Kleinfeld, 1986; Kleinfeld & Storch, 1993), the bilirubin metabolism (Zucker et al., 1992), and the action mechanism of biological probes (Clarke & Apell, 1989). The dynamics of porphyrins within membranes is also pertinent to heme biosynthesis (Cannon et al., 1984; Light & Olson, 1990). Lipidic, unilamellar vesicles were used as useful and reliable models making it possible to explore various aspects using spectroscopic and physicochemical methods (Blum & Grossweiner, 1985; Ricchelli et al., 1991).

In the present paper, using a stopped-flow apparatus with fluorescence detection, we investigated the kinetics of the interaction of a well-characterized dicarboxylic porphyrin, deuteroporphyrin, with dimyristoylphosphatidylcholine unilamellar vesicles of various sizes. In addition to direct studies on the incorporation of the porphyrin in vesicles, its transfer from vesicles to albumin, an efficient porphyrin carrier, is investigated in detail. Exhaustive theoretical analysis of the

† This work was supported by a grant from the French government to K.K.

® Abstract published in *Advance ACS Abstracts*, July 15, 1994.

0006-2960/94/0433-9447$04.50/0

kinetics as well as the effects of temperature and cholesterol allow us to characterize the movement of the porphyrin between the inner and outer leaflet of the bilayer in addition to the entrance in the vesicle and the exit in the bulk aqueous medium.

MATERIALS AND METHODS

Measurements. Emission and excitation fluorescence spectra were recorded using a SPEX spectrofluorimeter (Edison, NJ). Fluorescence emission was excited at 400 nm. The excitation spectra were recorded with the emission monochromator set at the emission maximum. A long-pass filter (420 nm) was put in front of the emission monochromator to remove scattered light. The porphyrin concentration was generally 3×10^{-8} M, and the temperature was 32 °C.

Kinetic measurements were performed with the aid of a Durrum–Gibson stopped-flow apparatus (Palo Alto, CA) with a mixing time of 3 ms. The excitation light was provided by a 75-W short-arc xenon lamp. The excitation monochromator was generally set at 408 or 389 nm to follow the incorporation of DP[1] in vesicles or the transfer of DP from vesicles to albumin, respectively. A filter cutting off light below 610 nm (Schott OG 610, Mainz, Germany) was put in front of the photomultiplier in order to remove scattered light and, in the first set of experiments, to reduce the contribution of nonincorporated porphyrin to the fluorescence. The signal was recorded using a digital oscilloscope (Nicolet Model 3091, Madison, WI) and then fed to a computer (Hewlett-Packard Model 9816, Fort Collins, CO). The signals were fitted by mono- or biexponential curves using a program based on the least-squares method. The quality was assessed from the χ^2 value (Press et al., 1988) and by fitting residuals. Curves were interpreted as monoexponential when biexponential fits led to essentially the same shape for the residuals and did not result in significant reduction in the χ^2 value (i.e., χ^2 monoexponential/χ^2 biexponential < 1.2). On the other hand, for biphasic processes, biexponential fit did reduce the χ^2 value (at least 5 times) and led to much better random distribution of residuals. Typical examples are shown in Figures 4 and 6. The errors indicated for the values of the rate constants represent the standard deviations of several measurements.

Chemicals. All the experiments were performed using 0.15 M NaCl solutions buffered to pH 7.4 with 20 mM Tris. Dimyristoylphosphatidylcholine (DMPC) and lipid-free human serum albumin (HSA) were purchased from Sigma Chemical Co. (St. Louis, MO). Cholesterol was obtained from Aldrich Chemical Co. (Milwaukee, WI). Sepharose 4B and Sepharose 2B were purchased from Pharmacia (Uppsala, Sweden). Deuteroporphyrin (DP), the structure of which is shown in Figure 1, was prepared in our laboratory as described elsewhere (Brault et al., 1986). Its purity, as checked by HPLC (Dellinger & Brault, 1987), was determined to be better than 99%. A stock solution of DP was prepared in freshly distilled tetrahydrofuran (THF) and kept in the dark at −18 °C. Intermediate solutions were obtained by mixing this stock solution with buffer. They were used without delay to prepare the final diluted solutions. The latter were renewed frequently. This procedure was found to minimize aggregation and loss of material due to adsorption of the porphyrin on glass. The porphyrin solutions were handled in the dark, and the stability was checked periodically by spectrofluorimetry.

[1] Abbreviations: DMPC, dimyristoylphosphatidylcholine; DP, deuteroporphyrin; HSA, human serum albumin; SUV, small unilamellar vesicles; THF, tetrahydrofuran.

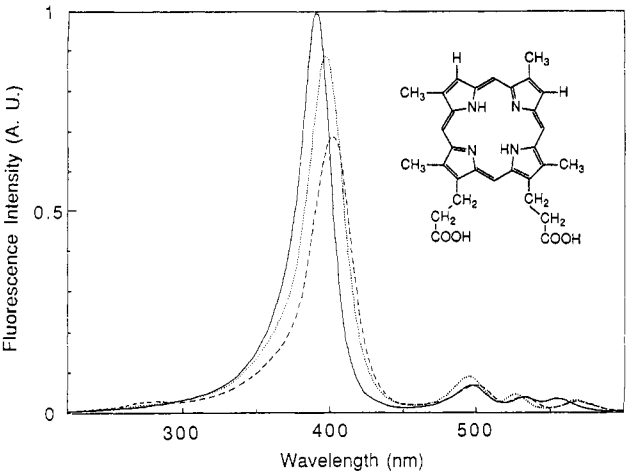

FIGURE 1: (Inset) Structure of deuteroporphyrin. Fluorescence excitation spectra of 3×10^{-8} M deuteroporphyrin in different environments at 32 °C: (—) aqueous solution buffered at pH 7.4, emission wavelength 609.5 nm; (· · ·) vesicle solution, [DMPC] = 8×10^{-4} M, emission wavelength 621.5 nm; (– –) albumin solution, [HSA] = 5×10^{-6} M, emission wavelength 623 nm.

Vesicle Preparation. Small unilamellar vesicles made of either pure DMPC or DMPC:cholesterol mixtures (1:1 molar ratio) were essentially prepared by extrusion (Olson et al., 1979; Mayer et al., 1986; Nayar et al., 1989). The lipid solutions in chloroform:methanol (9:1) were taken to dryness and then dispersed in buffer by vortexing. The resulting liposome suspension was extruded through a stack of two polycarbonate membrane filters (Poretics Corp., Livermore, CA) using an extruder device (Lipex Biomembranes, Vancouver, Canada) thermostated at 32 °C. The pore diameter was 0.05, 0.1, or 0.2 μm. In the case of mixed DMPC: cholesterol vesicles, the solution was preextruded through membranes with 0.2-μm pores. After 6–10 passages of the solutions through the filters, no more large liposomes remained as controlled by column chromatography on Sepharose 2B.

In some cases, vesicles were prepared by sonication. The aqueous dispersion of lipids prepared as described above was sonicated under argon using a sonifier (Branson Model B15, Danbury, CT) until clear solutions were obtained. The sonicated solutions were passed through a Sepharose-4B column (2.5 × 40 cm). The elution was followed by right angle light scattering using a Shimadzu fluorimeter RF 535 (Kyoto, Japan). The expected profile with a small contribution of large liposomes (Huang, 1969) was observed. Only the top fraction corresponding to the SUV peak was collected.

Size distributions and diffusion coefficients of vesicles were determined by quasi-elastic light scattering using a Coulter N4M analyzer (Hialeah, CA). The diameters of the vesicles are given in Table 1. For extruded vesicles, only one population of vesicles with a narrow size distribution was found. Sonicated vesicles contained a few percent of larger vesicles. The concentration of vesicle solutions was measured by the phosphorus assay method (Bartlett, 1959).

Incorporation of Porphyrin in Vesicles. For experiments at equilibrium, 10-μL aliquots of a 6×10^{-6} M DP solution in a THF:buffer mixture (1:10) were added to solutions (2 mL) containing various amounts of vesicles. They were incubated for 20 min at 32 °C before the fluorescence spectra were recorded. Then, 10 μL of Triton X-100 was added, and the spectra were recorded again. This step led to disruption of the vesicles and solubilization of all the porphyrin in Triton micelles. A fluorescence signal proportional to the total porphyrin concentration was thus obtained. This made it

Table 1: Interactions of Deuteroporphyrin with DMPC Vesicles (pH 7.4, 32 °C): Characteristic Constants

vesicles preparation[a]	diameter (nm)	$k_{on} \times 10^{-6}$ (M^{-1} s^{-1})	$k_{on} \times 10^{-10}$ (ves^{-1} s^{-1})	k_{off} (s^{-1})	$K_L^{eq} \times 10^{-4}$ (M^{-1})	$K_L^{kin} \times 10^{-4}$ (M^{-1})	$k_{ti} + k_{to}$ (s^{-1})	k_{to} (s^{-1})
sonicated	38 ± 4	3.5 ± 0.4	3.6 ± 0.4	39 ± 2	7.8 ± 1.7	15.3 ± 2.5	1.4 ± 0.2	0.7 ± 0.1
extruded (50)	63.5 ± 1.5	1.75 ± 0.05	5.30 ± 0.15	21.5 ± 1.5	14 ± 2	14.6 ± 1.5	0.8 ± 0.1	0.4 ± 0.1
extruded (100)	105 ± 4	1.05 ± 0.15	9.2 ± 1.3	18.5 ± 1.5	12 ± 2	10.7 ± 2.4	0.9 ± 0.3	0.4 ± 0.1
extruded (200)	222 ± 10	0.75 ± 0.1	30 ± 4	13.3 ± 1.0	12 ± 2	11.0 ± 2.3	0.9 ± 0.3	0.4 ± 0.1

[a] The number in parentheses corresponds to the diameter of membrane pores (in nm). The given diameters are the mean values and standard deviations calculated from three measurements. k_{on} (in M^{-1} s^{-1}) was obtained from the incorporation measurements. k_{on} (in ves^{-1} s^{-1}) (i.e., per mole of vesicles) was calculated assuming that the area per lipid head was 0.75 nm^2 and the bilayer thickness was 3 nm (Watts et al., 1978). k_{off} given here was obtained from the transfer measurements which are more precise. They agree with the values of k_{off} calculated from the incorporation measurements. K_L^{eq} and K_L^{kin} are the constants derived from measurements at equilibrium and calculated using rate constants, respectively. $k_{to} + k_{ti}$ was obtained from the incorporation measurements. k_{to} was obtained from the transfer measurements.

possible to correct the fluorescence spectra for small differences in porphyrin concentration.

The porphyrin solutions used in kinetics experiments were prepared just before they were mixed with the vesicles in the stopped-flow apparatus. The final concentration of DP after mixing was 1×10^{-7} M. Typically, the porphyrin solutions were made by adding 33 μL of a 6×10^{-5} M DP solution in a THF:buffer mixture to 10 mL of buffer. If not specified, the amount of THF in the solution did not exceed 0.04% (vol/vol).

Transfer of Porphyrin from Vesicles to Albumin. Solutions of DP prepared as indicated above were first incubated for 1 h with preformed vesicles at room temperature, in the dark. Then, they were mixed in the stopped-flow apparatus with solutions of albumin in buffer. The same kinetics results were obtained when the porphyrin was added to the phospholipids prior to the vesicle formation.

Experiments at equilibrium were performed in a similar way, except that the vesicle–porphyrin–albumin mixtures were allowed to equilibrate for about 15 min before the spectra were recorded.

Theoretical Models. The schemes presented below have a bearing on the incorporation of heme in vesicles and the transfer of heme from vesicles to proteins which were previously examined by Cannon et al. (1984) and Light and Olson (1990). However, these authors *a priori* assumed that the steps were well separated in time so that equilibria can be considered independent of each other, which represents a crude approximation. Here, we develop a comprehensive treatment leading to general expressions. If helpful, and if justified, simplified relations are derived afterwards. In our framework, the equilibrium constants are obtained from the kinetics expressions as special cases.

(A) Incorporation of Porphyrin in Vesicles. One-step incorporation of dyes in vesicles has been considered in detail by Clarke and Apell (1989). Provided the phospholipid concentration is large compared to that of the dye, it can be assumed that the state of occupancy of a vesicle does not influence the interaction with further dye molecules. In these conditions, the system can be simply described by focusing on the dye in its various environments. Moreover, the association step can be considered as a pseudo-first-order process. These conditions prevail in our experiments. Indeed, the smallest concentration of DMPC used was 5×10^{-6} M. With a DP concentration of 1×10^{-7} M and an affinity constant of 1.4×10^5 M^{-1}, for instance (see Results), it can be calculated that the lipid:porphyrin ratio is at least 100 in the least favorable case. As a matter of fact, a further decrease of the porphyrin concentration did not change the kinetics observed.

Here, we will consider a two-step mechanism for the incorporation of the porphyrin in the vesicles: (i) bimolecular interaction of the porphyrin with a vesicle leading to incorporation in the outer lipidic layer and (ii) partition of the porphyrin between the outer and inner layers. It is not assumed that these steps are separated in time, *a priori*. Denoting P_f, P_o, and P_i as the concentrations of DP free in the bulk aqueous solution, incorporated in the outer leaflet, or incorporated in the inner leaflet, respectively, and assuming that binding is a pseudo-first-order process, we have Scheme 1

Scheme 1

$$P_f \underset{k_{off}}{\overset{k_{on}'}{\rightleftarrows}} P_o \underset{k_{to}}{\overset{k_{ti}}{\rightleftarrows}} P_i$$

where $k_{on}' = k_{on}[\text{DMPC}]$.

(i) Kinetics. The kinetics of the process are then described by a system of equations as follows:

$$\frac{dP_f}{dt} = -k_{on}'P_f + k_{off}P_o$$

$$\frac{dP_o}{dt} = k_{on}'P_f - (k_{off} + k_{ti})P_o + k_{to}P_i \quad (1)$$

$$\frac{dP_i}{dt} = k_{ti}P_o - k_{to}P_i$$

where k_{on}' and k_{off} are the rate constants for porphyrin binding to the outer layer and exit from the outer layer; k_{ti} and k_{to} are the rate constants for migration toward the inner and the outer monolayer, respectively.

In the most general case, for a system of n successive reversible reactions, the evolution of the concentrations of all components as a function of time is described by a set of expressions comprising constant terms and n exponential terms with the same exponential factors (Rakowski, 1906), for example, in our case:

$$P_f = A_1 + B_1 \exp(-k_1 t) + C_1 \exp(-k_2 t)$$

$$P_o = A_2 + B_2 \exp(-k_1 t) + C_2 \exp(-k_2 t) \quad (2)$$

$$P_i = A_3 + B_3 \exp(-k_1 t) + C_3 \exp(-k_2 t)$$

In the range of porphyrin concentrations used, no inner screen effect can occur, and the fluorescence signal emitted by each form of DP is directly proportional to its concentration (Margalit & Rotenberg, 1984). The total fluorescence intensity F is the sum of all contributions. Thus, the observed fluorescence signal can be written as a sum of one constant and two exponential terms with the rate constants k_1 and k_2 defined in the above expressions.

Using Laplace transforms, k_1 and k_2 can be calculated to be (see Appendix):

$$k_{1,2} = \frac{1}{2}\left(\sum k \pm [(\sum k)^2 - 4(k_{on}'k_{ti} + k_{off}k_{to} + k_{on}'k_{to})]^{1/2}\right) \quad (3)$$

where $\sum k = k_{on}' + k_{off} + k_{ti} + k_{to}$. As detailed in the Appendix, further development, substitution, and disregard of small terms (errors resulting from approximations are discussed below) give

$$k_1 = k_{on}[\text{DMPC}] + k_{off} + k_{to} + k_{ti} \quad (4)$$

$$k_2 = k_{to} + k_{ti} \quad (5)$$

(ii) Equilibrium State. The distribution of the porphyrin at equilibrium can also be calculated from the system of eq 1 as a special case. Indeed, at equilibrium

$$\frac{dP_f}{dt} = \frac{dP_o}{dt} = \frac{dP_i}{dt} = 0$$

which yields

$$P_i = \frac{k_{ti}}{k_{to}} P_o \quad \text{and} \quad P_f = \frac{k_{off}}{k_{on}'} P_o$$

Considering together the porphyrin molecules incorporated either in the inner or the outer leaflets of the vesicles, an overall association constant can be defined as

$$K_L = \frac{(P_i + P_o)}{P_f[\text{DMPC}]}$$

It is easily shown that

$$K_L = (1 + k_{ti}/k_{to})k_{on}/k_{off} \quad (6)$$

At a given wavelength and for a fixed porphyrin concentration, the equilibrium constant can be derived (Brault et al., 1986) from

$$F = F_0 + (F_{\text{DMPC}} - F_0)\frac{K_L[\text{DMPC}]}{1 + K_L[\text{DMPC}]} \quad (7)$$

where F_0 and F_{DMPC} are the fluorescence intensities corresponding to no and full incorporation of the porphyrin in the vesicle lipidic phase, respectively.

(B) Transfer of Porphyrin from Vesicles to Albumin. In keeping with previous studies on molecules solubilized in vesicles (Almgren, 1980; Storch & Kleinfeld, 1986; Light & Olson, 1990; Zucker et al., 1992), it is assumed that the transfer of the porphyrin to albumin occurs via the aqueous phase. In our experimental conditions, the albumin concentration greatly exceeds that of the porphyrin and Scheme 2 will hold

Scheme 2

$$P_i \underset{k_{ti}}{\overset{k_{to}}{\rightleftarrows}} P_o \underset{k_{on}'}{\overset{k_{off}}{\rightleftarrows}} P_f \underset{k_{dis}}{\overset{k_{as}'}{\rightleftarrows}} P_b$$

where P_b is the concentration of DP bound to albumin; P_i, P_o, and P_f are as described above; $k_{as}' = k_{as}[\text{HSA}]$.

(i) Kinetics. The system is described by the following equations:

$$\frac{dP_i}{dt} = k_{ti}P_o - k_{to}P_i$$

$$\frac{dP_o}{dt} = k_{to}P_i - (k_{ti} + k_{off})P_o + k_{on}'P_f$$

$$\frac{dP_f}{dt} = k_{off}P_o - (k_{on}' + k_{as}')P_f + k_{dis}P_b \quad (8)$$

$$\frac{dP_b}{dt} = k_{as}'P_f - k_{dis}P_b$$

with the initial conditions $P_i(0) = P_i^0$, $P_o(0) = P_o^0$, and $P_f(0) = P_b(0) = 0$.

According to the above-mentioned rule, in the most general case the solution of this system will involve three exponential terms with complex analytical expressions. However, a considerable simplification can be obtained by considering the experimental conditions which will prevail in our study. Indeed, owing to the concentrations of vesicles and albumin used, the rates for the association of DP with albumin or vesicles are much larger than the exit rates to aqueous solution. The concentration of the free form (P_f) will remain very low (<1%), which was in fact an important requirement in designing this study (see Discussion). In these conditions, the steady-state method of Bodenstein (Benson, 1960) holds, i.e., with the exception of a short initial period, $dP_f/dt = 0$. We can thus express P_f as a function of P_o and P_b and transform the system into

$$\frac{dP_i}{dt} = \beta P_o - \alpha P_i$$

$$\frac{dP_o}{dt} = \alpha P_i - (\beta + \gamma)P_o + \delta P_b \quad (9)$$

$$\frac{dP_b}{dt} = \gamma P_o - \delta P_b$$

where $\alpha = k_{to}$, $\beta = k_{ti}$, $\gamma = (k_{off}k_{as}')/(k_{on}' + k_{as}')$, and $\delta = (k_{dis}k_{on}')/(k_{on}' + k_{as}')$.

This system of equations has a form similar to that given above and yields solutions consisting of constants and two exponential terms with rate constants equal to

$$k_{1,2} = \frac{(\alpha + \beta + \gamma + \delta) \pm [(\alpha + \beta + \gamma + \delta)^2 - 4(\alpha\gamma + \beta\delta + \alpha\delta)]^{1/2}}{2} \quad (10)$$

These rate constants are predicted to depend on the concentrations of vesicles and albumin as γ and δ do. Although eq 10 is quite complex, the main features can be illustrated by considering limiting conditions.

When the albumin concentration is low compared to that of vesicles ($k_{on}' \gg k_{as}'$ and $\delta \gg \gamma$), eq 10 reduces to

$$k_{1,2} = \frac{\alpha + \beta + \delta \pm (\alpha + \beta - \delta)}{2}$$

$$k_1 = \delta = k_{dis} \quad (11)$$

$$k_2 = \alpha + \beta = k_{to} + k_{ti} \quad (12)$$

At high albumin concentration ($k_{as}' \gg k_{on}'$ and $\gamma \gg \delta$), eq 10 reduces to

$$k_{1,2} = \frac{\alpha + \beta + \gamma \pm [(\beta - \alpha + \gamma)^2 + 4\alpha\beta]^{1/2}}{2}$$

In the present experiments, the transfer of the porphyrin across the bilayer was much slower than the dissociation from the vesicles, and the second-order term $\alpha \cdot \beta$ can be neglected yielding

$$k_{1,2} = \frac{\alpha + \beta + \gamma \pm (\beta - \alpha + \gamma)}{2}$$

$$k_1 = \gamma + \beta = k_{off} + k_{ti} \quad (13)$$

$$k_2 = \alpha = k_{to} \quad (14)$$

The above calculations and numerical simulations (see Figure 7) show that k_1 smoothly varies between k_{dis} and $k_{off} + k_{ti}$. The rate constant k_2 is determined essentially by membrane crossing and ranges between k_{to} and $k_{to} + k_{ti}$.

The system (9) of kinetic equations can be used also for the description of the inverse process, i.e., the transfer of porphyrin from albumin to vesicles. It can be easily shown that the rate constants for this process are still given by eq 10. The only difference is in the initial conditions which are $P_b(0) = P_b^0$ and $P_o(0) = P_i(0) = P_f(0) = 0$. The amplitudes of the fast and the slow phases are modified accordingly.

(ii) Equilibrium State. As in the previous case, the distribution of the porphyrin at equilibrium can be derived from the system (eq 9) of kinetic equations. At equilibrium

$$\frac{dP_i}{dt} = \frac{dP_o}{dt} = \frac{dP_b}{dt} = 0$$

The set of relations (eq 9) allows us to calculate the fraction x of porphyrin incorporated in vesicles (not that it is assumed that no free porphyrin remains):

$$x = \frac{P_o + P_i}{P_o + P_i + P_b} = \frac{(1 + k_{ti}/k_{to})k_{on}[\text{DMPC}]/k_{off}}{(1 + k_{ti}/k_{to})k_{on}[\text{DMPC}]/k_{off} + k_{as}[\text{HSA}]/k_{dis}} \quad (15)$$

or

$$x = \frac{K_L[\text{DMPC}]}{K_L[\text{DMPC}] + K_A[\text{HSA}]} \quad (16)$$

where $K_A = k_{as}/k_{dis}$ (equilibrium constant for porphyrin binding to HSA) and K_L has the same definition as above.

It can be easily shown that

$$x = \frac{F - F_{HSA}}{F_{DMPC} - F_{HSA}} \quad (17)$$

where F_{HSA} and F_{DMPC} correspond to the fluorescence intensities of the porphyrin totally bound to albumin or fully incorporated in vesicles, respectively.

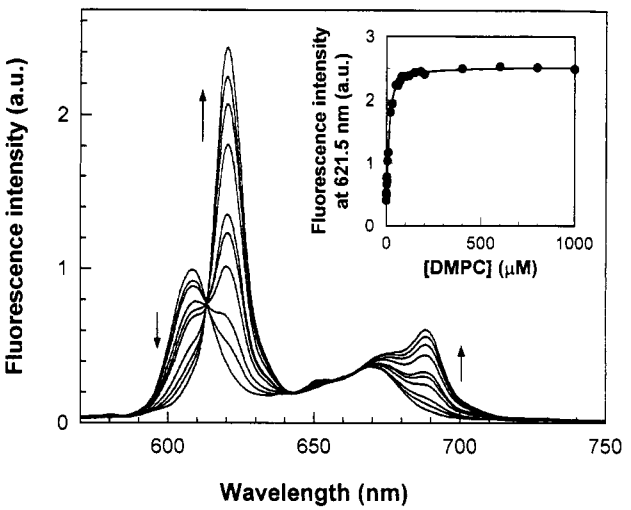

FIGURE 2: Examples of fluorescence emission spectra of 3×10^{-8} M deuteroporphyrin in the presence of different amounts of DMPC vesicles. Vesicles were prepared by extrusion on 50-nm pores. Excitation wavelength, 408 nm; temperature, 32 °C. The arrows indicate the direction of spectral changes when the vesicle concentration was increased. DMPC concentrations were 0, 0.5, 3, 6, 8, 10, 20, 30, 50, and 100 μM. (Inset) (●) Fluorescence intensity at 621.5 nm as a function of DMPC concentration; (—) theoretical curve drawn according to eq 7 with $K_L = 1.4 \times 10^5$ M^{-1}.

RESULTS

Steady-State Measurements

The fluorescence excitation spectra of DP in buffer, incorporated in vesicles or bound to HSA are shown in Figure 1. The two latter spectra were obtained by using a large excess of either vesicles ([DMPC] = 8×10^{-4} M) or albumin ([HSA] = 5×10^{-6} M), respectively. In each case, the emission monochromator wavelength was set to the maximum of porphyrin emission. DMPC does not fluoresce, and albumin fluorescence is negligible in the range of porphyrin emission. Although the use of a long-pass filter in stopped-flow experiments somewhat distorts these excitation profiles, their main features are maintained. In particular, the spectra appear to be different enough to easily follow changes in the porphyrin environment. It can be noted that the excitation spectra of DP bound to vesicles and to albumin intersect around 405 nm.

Equilibrium Measurements

The partition of DP between the lipidic phase of vesicles and the bulk aqueous phase was studied at 32 °C by recording the fluorescence emission spectra of solutions made with various lipid concentrations (0–1 $\times 10^{-3}$ M) and a constant porphyrin concentration (3×10^{-8} M). A typical set of spectra is given in Figure 2. As expected, it shows isoemissive points in agreement with the assumption that the contributions to the fluorescence of all the species are proportional to their concentrations (Brault et al., 1986). The spectrum obtained at the highest vesicle concentration is very similar, in shape and maximum emission wavelength, to that of DP in organic solvents. This indicates that, whatever the location of the porphyrin in the bilayer, the porphyrin core remains buried in a hydrophobic environment. Changes in fluorescence intensity were plotted according to eq 7 to determine the association constant K_L. A typical plot is shown in Figure 2 (inset) for vesicles made using membranes with 0.05-μm pores.

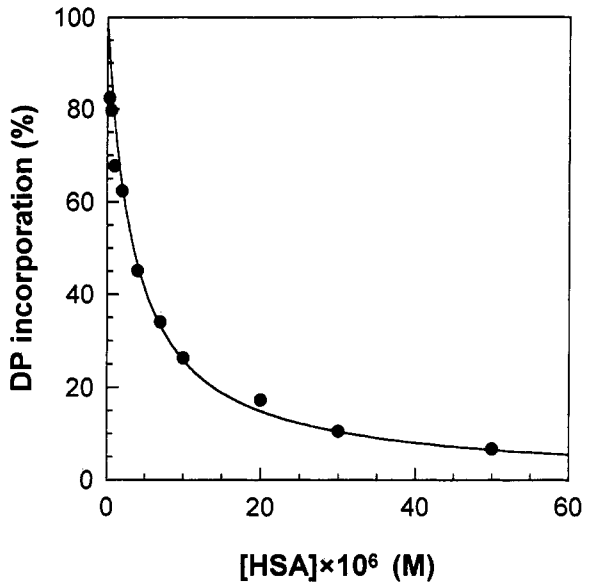

FIGURE 3: Distribution of deuteroporphyrin (3×10^{-8} M) between vesicles ([DMPC] = 1.3×10^{-3} M) and albumin calculated from fluorescence emission changes at 622 nm according to eq 17. Excitation wavelength, 389 nm; temperature, 32 °C. Theoretical curve (—) was drawn according to eq 16 with $K_L = 1.4 \times 10^5$ M^{-1} and $K_A = 5.2 \times 10^7$ M^{-1}.

The best fit was obtained with a K_L value of $(1.4 \pm 0.2) \times 10^5$ M^{-1}. The equilibrium constants obtained for vesicles of various sizes are listed in Table 1. For the sake of comparison and because lipid concentrations are determined with the best accuracy, the association constants (as well as kinetic constants determined below) are given in terms of phospholipid concentration rather than in terms of vesicle concentration.

In order to ascertain that no artifact could arise from vesicle fusion induced by DP, we followed the intensity of 300-nm light scattered at right angle in the spectrofluorimeter. The DMPC and DP concentrations were 1.3×10^{-3} and 1×10^{-7} M, respectively. No changes were observed after up to 4 h incubation at 32 °C, neither for the control vesicle solution nor for the DP–vesicle mixture. No changes were either observed even after 5 days. Control experiments showed that 10% fusion would be detected using this procedure.

The partition, at equilibrium, of DP between vesicles and albumin was studied by adding various amounts of HSA to solutions of vesicles preloaded with the porphyrin ([DMPC] = 1.3×10^{-3} M, [DP] = 3×10^{-8} M). The vesicle concentration was chosen so that at least 99.5% of the porphyrin was incorporated. The mixture was incubated at 32 °C for 10 min. The fluorescence emission spectra with excitation at 389 nm were recorded before and after addition of HSA. The fluorescence intensity was corrected to a small inner filter effect due to HSA absorption using ϵ(389 nm) = 700 M^{-1} cm^{-1}. The fraction of DP incorporated in vesicles was calculated according to eq 17 and was fitted according to eq 16. In Figure 3 is shown a typical plot obtained for 50-nm vesicles using the following values: $K_L = 1.4 \times 10^5$ M^{-1} and $K_A = 5.2 \times 10^7$ M^{-1}. The latter value is in excellent agreement with data obtained by Rotenberg et al. (1987).

Kinetic Measurements

Interaction of DP with Vesicles. When DP solutions were rapidly mixed with vesicles, we observed a biphasic signal which was best fitted by two exponentials. A typical curve is shown in Figure 4. The two phases are largely separated in time so that the first phase can be, in most cases, conveniently

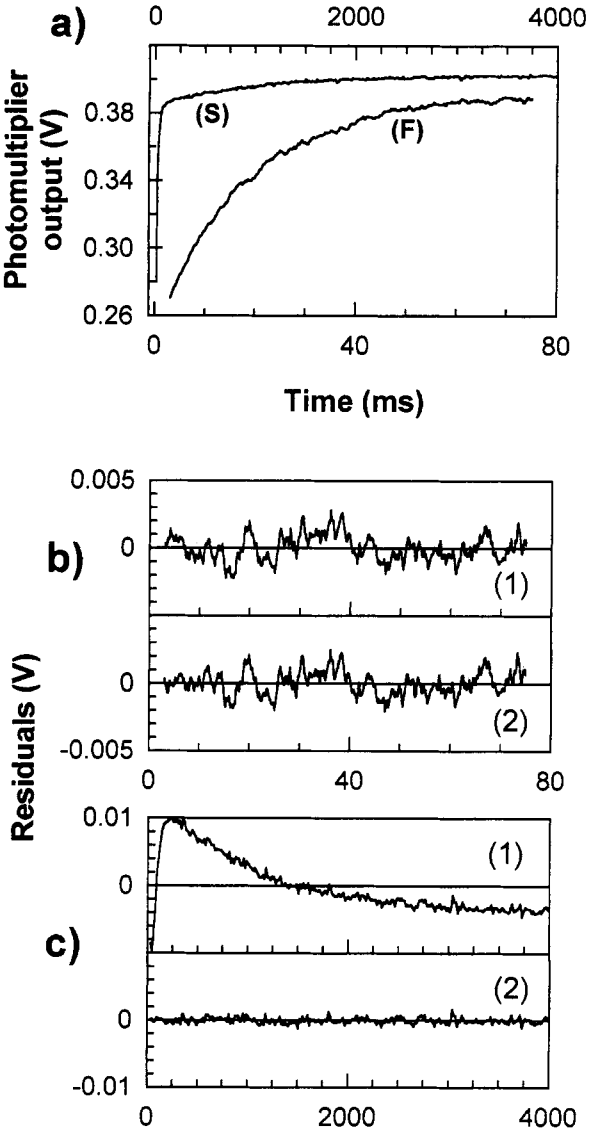

FIGURE 4: (a) Fluorescence intensity changes recorded upon mixing DMPC vesicles (final concentration: 2×10^{-5} M) with deuteroporphyrin (1×10^{-7} M): (F) fast phase (lower time scale); (S) slow phase (upper time scale); temperature, 32 °C; excitation wavelength, 410 nm. Vesicles were made by extrusion on 50-nm pores. (b) Deviations of the fast signal from the best monoexponential fit (1) and from the best biexponential fit (2). χ^2 monoexponential/χ^2 biexponential = 1.15. (c) Deviations of the slow signal from the best monoexponential fit (1) and from the best biexponential fit (2). χ^2 monoexponential/χ^2 biexponential = 80.

characterized using a monoexponential fit (see Figure 4). The rate constant of the first phase increased linearly with the concentration of DMPC (see Figure 5). Experimental values were best fitted by straight lines. As the amplitude of the signal also increased with DMPC concentration, it was feasible to extract the highest rate constant with reasonable confidence even when 1–2 half-times have elapsed during mixing time. The number of data points of the kinetic trace which were taken into account was reduced accordingly. As a consequence, the accuracy on the highest rate constants was less. For the 50-nm vesicles at 32 °C, the slope was found to be 1.73×10^6 M^{-1} s^{-1}, and the intercept was 22.4 s^{-1} (see Figure 5).

The rate constant of the second phase remained almost independent of the vesicle concentration except for the lower values (see Figure 5). As discussed below, the increase of the rate constant was likely to be due to the influence of THF.

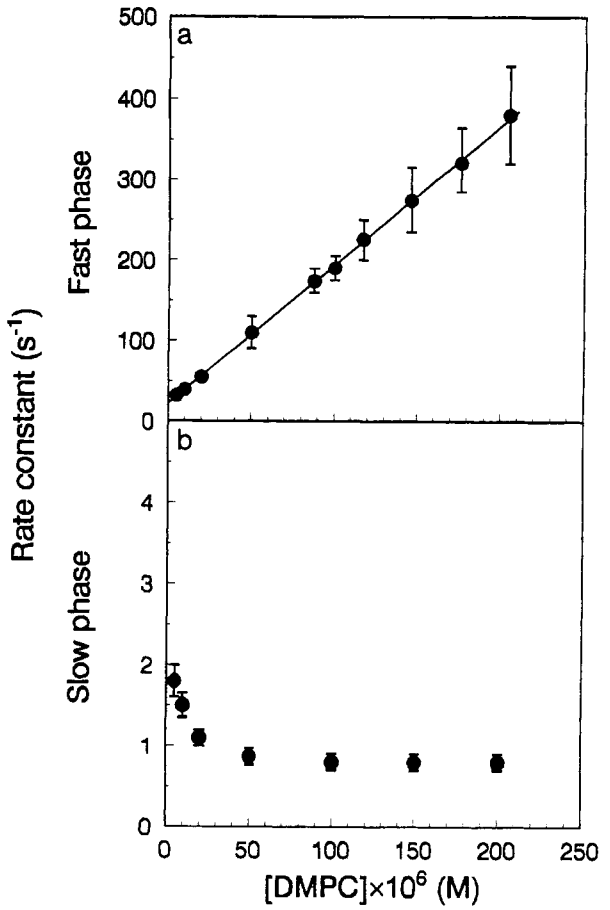

FIGURE 5: Rate constants of incorporation of deuteroporphyrin (1×10^{-7} M) into vesicles made by extrusion on 50-nm pores. Influence of DMPC concentration on (a) the fast phase and (b) the slow phase at 32 °C. Each point corresponds to the mean and the standard deviation calculated from 10 to 20 rate constant determinations.

The kinetics obtained with vesicles of other sizes were quite similar and were always characterized by two phases.

The ratio of the amplitude of the slow phase over that of the fast phase was generally of about 0.3 for the lowest vesicle concentrations and decreased steeply for the highest concentrations. It was less than 0.05 for [DMPC] = 2×10^{-4} M.

Transfer of DP from Vesicles to Albumin. Solutions of vesicles preloaded with DP were rapidly mixed with solutions containing various amounts of HSA. When excited at 389 nm, the fluorescence was found to decay in two well-defined exponential phases with roughly equal amplitudes. A typical curve is shown in Figure 6. When excitation was performed at 410 nm, the fluorescence increased, but the rate constants and the relative amplitudes of the two phases remained unchanged. The inversion of the fluorescence signal was observed at the same excitation wavelength for the two phases. This wavelength (around 403 nm) corresponded to the isoemissive point of DP incorporated in vesicles or bound to albumin (see Figure 1).

The rate constant of the first (fast) phase was found to depend on the concentrations of both DMPC and HSA. The dependence on HSA is shown in Figure 7 for two different concentrations of vesicles extruded on 50-nm pores. The curves are characterized by a common intercept for [HSA] = 0 and level off for the highest albumin concentrations. The temperature was 32 °C. The biexponential fit led to more uncertainty in the values of the rate constant of the second (slow) phase. At 32 °C, experimental values ranged between 0.35 and 0.7 s^{-1} for the extruded vesicles and between 0.6 and 1 s^{-1} for the sonicated ones. In each case, the lower values were obtained for the highest concentrations in albumin (see Figure 7).

The inverse transfer process (i.e., from albumin to vesicles) was also investigated as a control using vesicles extruded on 50-nm pores. The concentrations were [DMPC] = 2×10^{-3} M, [HSA] = 5.7×10^{-6} M, and [DP] = 1×10^{-7} M. The temperature was 32 °C. The porphyrin was incubated with albumin for 1 h in the dark, and the solution was then mixed with vesicles. An increasing two-exponential fluorescence signal (excitation wavelength 389 nm) was observed with $k_1 = 5.5 \pm 0.5$ s^{-1} and $k_2 = 0.62 \pm 0.05$ s^{-1}.

Changing the temperature had a drastic effect on the rate constants, as shown in Figure 8a–c. For all the vesicle concentrations investigated, the change in the rate of the slower process (Figure 8b) was particularly abrupt around the temperature of phase transition of DMPC (Watts et al., 1978). Below this temperature, it was too slow (<0.05 s^{-1}) to be studied with our apparatus. The effect on the fast phase was also important, but it almost vanished at the lowest albumin concentration (see Figure 8a and Discussion). Although Arrhenius plots are currently used in similar experiments and would yield linear representation, interpretation in terms of activation energies would be meaningless as several unrelated steps are involved in our systems. Direct plots were thus preferred.

Quite different behavior was displayed by vesicles made of a DMPC:cholesterol mixture (1:1). Only a fast monoexponential signal remained with no more evidence of the slow component. As shown in Figure 8c, the effect of temperature was less important than in the former case.

Although the amount of tetrahydrofuran (which aided in preparation of porphyrin solutions) was low in the final solutions used for experiments, we tested its effect on the kinetics. The results are shown in Figure 9. The fast phase was almost unaffected. The effect on the slow phase was more important, but it remained insignificant in most of our experimental conditions that involved a THF content lower than 0.04% (vol/vol). To further check this point, we also studied the transfer in a THF-free system. An aliquot of deuteroporphyrin in THF was added to a chloroform:methanol DMPC solution, then the solvent was evaporated to dryness and vesicles were prepared as usual. The two rate constants for the transfer of DP to albumin were found to match exactly those predicted by extrapolation of the data obtained with the THF-containing system (see Figure 9).

DISCUSSION

In keeping with previous results on sonicated egg phosphatidylcholine vesicles (Brault et al., 1986) or related studies (Ricchelli et al., 1991), the emission and excitation fluorescence spectra of DP bound to DMPC vesicles are indicative of a lipidic environment. Indeed, very similar spectra are recorded when this porphyrin is dissolved in an organic solvent (THF, chloroform). The incorporation of the porphyrin within DMPC vesicles was found to obey simple equilibrium laws as shown by the effect of increasing vesicle concentration on the fluorescence spectra (see Figure 2). Equilibrium constants determined at 32 °C (see Table 1) are almost independent of the vesicle size when expressed in terms of phospholipid concentration.

Owing to the asymmetrical structure of DP, it can be postulated that a particular orientation of the molecule within the lipidic bilayer is favored, the carboxylic acid side chains most likely interacting with the polar heads of the phospholipids

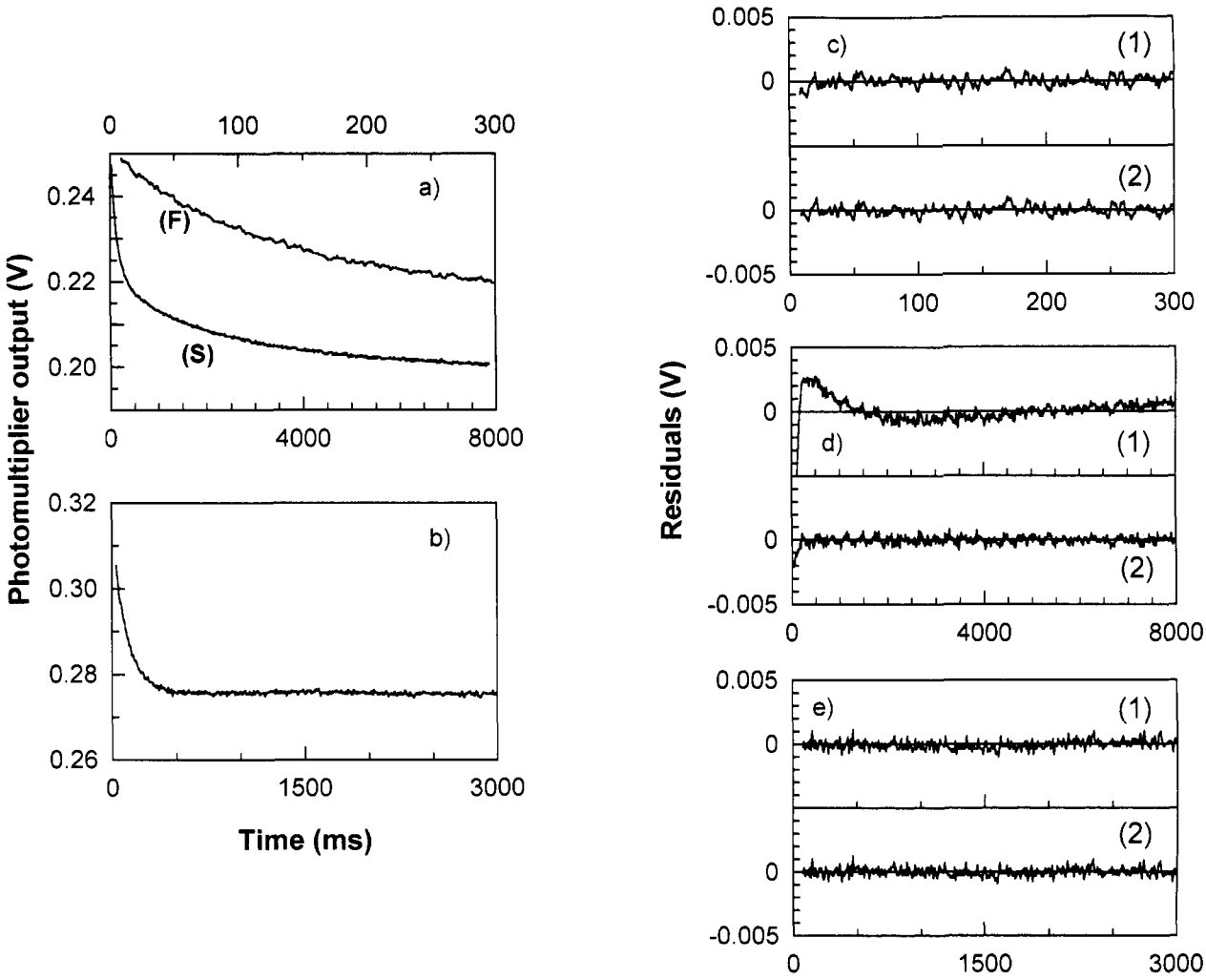

FIGURE 6: Fluorescence intensity changes recorded upon mixing vesicles preloaded with deuteroporphyrin (final concentration after mixing, DP = 1×10^{-7} M) and albumin: temperature, 32 °C; excitation wavelength, 389 nm. Vesicles were made by extrusion on 50-nm pores. (a) DMPC vesicles (final concentrations: [DMPC] = 1.3×10^{-3} M, [HSA] = 2×10^{-5} M). The traces (F) (upper time scale) and (S) (lower time scale) show the fast and the slow phases, respectively. (b) DMPC:cholesterol (1:1) vesicles ([DMPC] = [cholesterol] = 1×10^{-3} M, [HSA] = 5×10^{-5} M). (c and d) Deviations of the traces (F) and (S) from the best monoexponential fits (1) and from the best biexponential fits (2), respectively. χ^2 monoexponential/χ^2 biexponential were 1.03 and 40 for the traces (F) and (S), respectively. (e) Deviations of the trace shown in (b) from the best monoexponential fit (1) and from the best biexponential fit (2). The ratio χ^2 monoexponential/χ^2 biexponential was 1.09.

(Cannon et al., 1984). The porphyrin can be located with such an orientation either in the outer or in the inner leaflet of the bilayer [for a figure drawn to scale, see Brault (1990)]. The porphyrin is expected to present very similar fluorescence spectra in these two situations, and no information on the partition of the porphyrin between the two leaflets can be derived from steady-state measurements. The existence of two lipidic locations of the porphyrin is strongly suggested however, by kinetics. In all cases, we recorded a biphasic signal characterized by fluorescence changes in the same direction for both phases whatever the excitation wavelength was. These findings are best explained by assuming a fast binding of the porphyrin to the outer leaflet of the vesicle followed by a slower migration through the bilayer (see Scheme 1). The linear dependence of the first-phase rate constant on the phospholipid concentration and the presence of a slower phase support this scheme according to eqs 4 and 5, which allowed us to calculate k_{on}, k_{off}, and $k_{ti} + k_{to}$. The rate constants k_{on} were expressed either with regard to phospholipid concentration (in M^{-1} s^{-1}) or, knowing the vesicle size, in ves^{-1} s^{-1} units (i.e., per mole of vesicles). They are summarized in Table 1 for measurements made at 32 °C with vesicles of various sizes. The rate constants expressed in ves^{-1} s^{-1} show a remarkable linear dependence on the vesicle radius. This dependence on size strongly suggests that the process is controlled by diffusion. In this case the rate constant should be (Atkins, 1990)

$$k_{on}(\text{dif}) = 4\pi RDN \qquad (18)$$

where R can be taken as the vesicle radius, D is the sum of the diffusion coefficient of the vesicle and the porphyrin, and N is Avogadro's number. As discussed previously (Vever-Bizet & Brault, 1993), the diffusion coefficient of DP is likely to range in the limits of $(2.4 \pm 1.0) \times 10^{-10}$ m^2 s^{-1}, which are values measured for a related porphyrin or derived from the Stokes–Einstein equation, respectively. The diffusion coefficient of the vesicles that is, at most, 1×10^{-11} m^2 s^{-1} can be neglected. A theoretical value, $k_{on}(\text{dif}) = R \times 1.7 \times 10^{18}$ M^{-1} s^{-1}, can be computed in excellent agreement with most of the experimental data (some discrepancy was observed for the vesicles with the highest radius).

The rate constant of the slow phase remained constant (0.8–1 s^{-1}) for lipid concentrations above 5×10^{-5} M, in agreement with Scheme 1 and eq 5. An unexpected increase was however observed (see Figure 5) for small liposome concentrations,

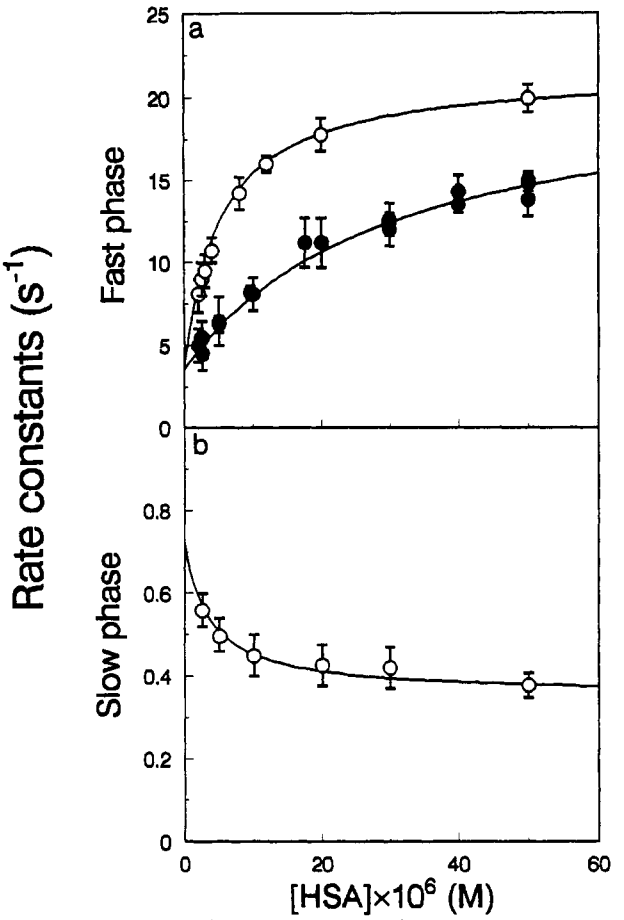

FIGURE 7: Transfer of deuteroporphyrin from DMPC vesicles to albumin. (a) Dependence of the experimental rate constant of the fast phase on albumin concentration. DMPC concentrations were 1.3×10^{-3} M (●) and 2×10^{-4} M (○). Each point corresponds to the mean and standard deviation calculated from 10 to 20 rate constant determinations. The figure includes the results from several independent experiments. (b) Dependence of the experimental rate constant of the slow phase on albumin concentration. DMPC concentration was 1×10^{-3} M. Each point corresponds to the mean of about 5 values. Other conditions are the same as in Figure 6. The full lines are theoretical curves calculated using eq 10 with the following values: $k_{on} = 1.73 \times 10^6$ M^{-1} s^{-1}, $k_{off} = 21.5$ s^{-1}, $k_{as} = 6.75 \times 10^7$ M^{-1} s^{-1}, $k_{dis} = 3.5$ s^{-1}, and $k_{ti} = k_{to} = 0.4$ s^{-1}.

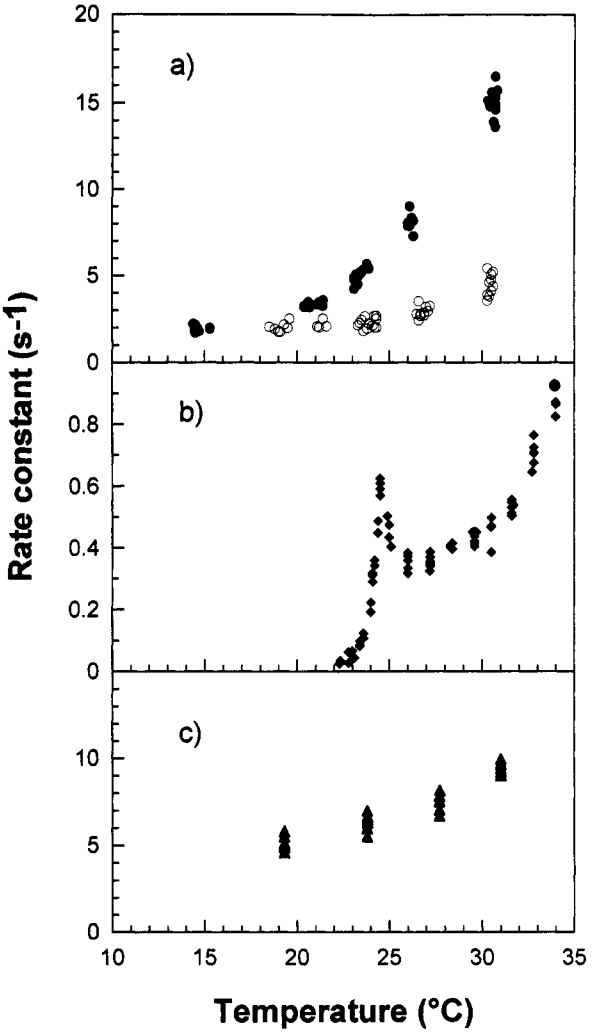

FIGURE 8: Effect of temperature on the rate constants of transfer of deuteroporphyrin (1×10^{-7} M) from vesicles to albumin. (a) Transfer from DMPC vesicles ([DMPC] = 1.3×10^{-3} M) to albumin ([HSA] = 5×10^{-5} M (●) or 2.6×10^{-6} M (○)): fast phase. (b) Transfer from DMPC vesicles (1.3×10^{-3} M) to albumin (5×10^{-5} M): slow phase. (c) Transfer from DMPC:cholesterol (1:1) vesicles ([DMPC] = [cholesterol] = 1×10^{-3} M) to albumin (5×10^{-5} M).

which does not fit our model (numerical simulations using eq 3 predict a slight decrease of the rate constant). This behavior is best explained by considering a possible effect of THF. As shown in Figure 9, THF has an accelerating effect on the kinetics, particularly on the slow phase. Although the content of THF was kept at a low value (0.04% vol/vol) in the experiments shown in Figure 5, the ratio between the amount of THF and that of DMPC might not be negligible for the lowest vesicle concentrations. In keeping with the effect of other solvents, such as dioxane (Blume, 1979), it is believed that THF has a fluidizing effect on the bilayer. This interpretation is fully consistent with the view that the slow phase mainly reflects bilayer crossing. Using the values obtained with the highest lipid concentrations, eq 5 allows us to derive $k_{ti} + k_{to} = 0.8 \pm 0.1$ s^{-1} for vesicles extruded on 50-nm pores. Values obtained with other vesicles were similar, with the exception of sonicated vesicles which yielded a somewhat higher value (this point is discussed below).

The values of $k_{ti} + k_{to}$ being known, those of k_{off} are computed from plots such as that shown in Figure 5 by using eq 4. They are summarized in Table 1. It was assumed in previous studies that both k_{on} and k_{off} were diffusion controlled and that the partition of the solubilized molecule did not depend on the vesicle size. If true, k_{off} should be inversely proportional to the radius of the vesicles according to Almgren (1980). In the present study, experimental values of k_{off} were obtained. Although they do show a significant decrease with the vesicle radius, an inverse dependence is not fully obeyed. Assuming $k_{ti} \approx k_{to} \approx k_t$, errors resulting from the approximation made to derive eqs 4 and 5 can be calculated to be 2% on k_{on}, 1.5% on k_{off}, and 6% on k_t. They do not exceed the experimental errors.

Although strong evidence for slow bilayer crossing is provided by the experiments discussed above, mixing the porphyrin with vesicles is not sufficient to extract all the pertinent constants. In particular, only the sum $k_{ti} + k_{to}$ can be obtained. Also, as experimentally confirmed, theoretical simulations (not shown) predict a decrease of the amplitude of the slow process when the lipid concentration increases, which might lead to difficulties in interpreting experimental data. Another point must be considered. Hydrophobic porphyrins are known to dimerize (Margalit & Rotenberg, 1984) and eventually aggregate or adsorb on glass, which might lead to spurious results. We therefore looked for a system making it possible to keep the porphyrin concentration in the aqueous medium to a negligible level.

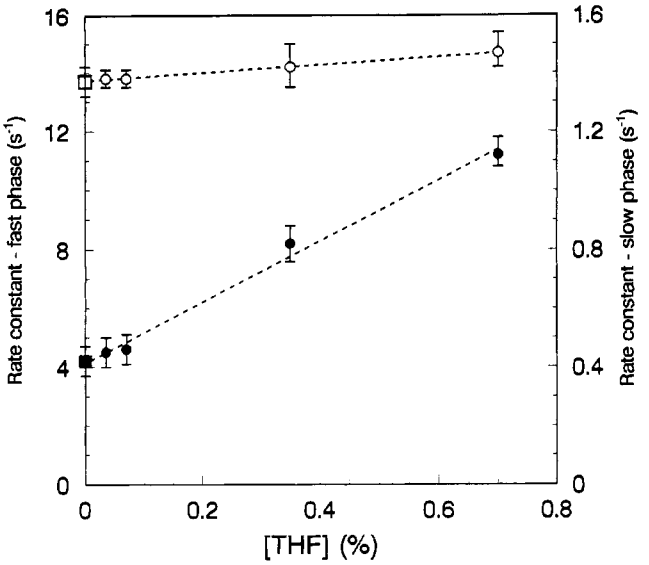

FIGURE 9: Effect of tetrahydrofuran (%, vol/vol) on the kinetics of transfer of deuteroporphyrin from DMPC vesicles to albumin. Vesicles were made by extrusion on 50-nm pores. Final concentrations were [DP] = 1×10^{-7} M, [DMPC] = 1.3×10^{-3} M, and [HSA] = 4×10^{-5} M. Open symbols, fast phase; filled symbols, slow phase. The porphyrin was added after (○, ●) or before (□, ■) vesicle formation. The dotted lines are the best linear fits of experimental data.

This was found by mixing albumin with vesicles preloaded with the porphyrin. Albumin is a well-known porphyrin carrier. A high-affinity binding site for monomeric deuteroporphyrin has been identified by means of spectrofluorimetry (Rotenberg et al., 1987). The related affinity constant ($K_A = 5 \times 10^7$ M^{-1}) was found to depend little on the temperature and was not affected by the presence of fatty acids bound to the protein. Other sites with lower affinity may also exist. In our experimental conditions, the vesicle concentration was always high enough to trap all the porphyrin molecules when no albumin was present. On the addition of albumin, redistribution of the porphyrin between liposomes and albumin takes place. As the albumin concentration was much larger than that of the porphyrin, only the high-affinity binding site is expected to be occupied, and pseudo-first-order binding kinetics will prevail. As shown in Figure 3, the distribution at equilibrium is determined only by the two association constants K_L and K_A, which govern the equilibria of DP with liposomes and albumin, respectively. Therefore, the distribution of DP is not influenced by possible interactions between HSA and vesicles or phospholipids. Other related studies also failed to detect any effect of such interactions (Daniels et al., 1985; Rotenberg et al., 1987).

The existence of two porphyrin pools moving from a lipidic environment to that provided by albumin is clearly evidenced by the biphasic character of the kinetics and the dependence of the signal on wavelength. The two components of the signal behaved in the same way and inverted at the same wavelength (see Results). It was assumed that these pools correspond to porphyrins located either in the inner or the outer leaflet of the bilayer and that the transfer to albumin takes place through the aqueous phase according to Scheme 2. In all our experimental conditions, the two components were well separated in time. As only the faster one was found to depend to an important extent on lipid and albumin concentration, there was no doubt as to the assignment of the two phases predicted by eq 10.

All the experimental data obtained either in the absence or in the presence of albumin were found to be consistent with the proposed schemes. In Figure 7a is shown the effect of albumin on the fast rate constant for two vesicle concentrations. The data on the effect of albumin were fitted according to eq 10 using the following values: k_{on} and k_{off} determined without albumin, k_{ti} and k_{to} determined by considering the slower step (see below). The best fits were obtained with values of $k_{as} = (6.75 \pm 0.75) \times 10^7$ M^{-1} s^{-1} and $k_{dis} = (3.5 \pm 1)$ s^{-1}. According to eq 11, the value of k_{dis} can be obtained with good accuracy from the intercept of the curves, independent of the lipid concentration used. Moreover, when experiments were performed using vesicles of other sizes or vesicles made of DMPC–cholesterol mixtures, the same intercept (i.e., the same value of k_{dis}) was obtained. The ratio $k_{as}/k_{dis} = 1.9 \times 10^7$ M^{-1} is somewhat different from the association constant $K_A = 5.2 \times 10^7$ M^{-1}. This might indicate that the formation of the porphyrin–albumin complex involves some steps in addition to the initial bimolecular interaction. However, we found no evidence for such an additional step by studying directly the interaction of DP with albumin using our stopped-flow apparatus (data not shown). Also, the rate constants derived from experiments involving the transfer of DP either from albumin to vesicles or from vesicles to albumin were found to be in excellent agreement (see below). As far as kinetics on the millisecond or second time scales are considered, a single binding site of DP on albumin appears to be involved. However, other binding sites characterized by slower association and dissociation rates could also exist, which might explain the difference between K_A and k_{as}/k_{dis}.

In Scheme 2, it is assumed that the transfer of the porphyrin takes place via the bulk aqueous solution. Direct transfer of the porphyrin on collision of the vesicles with albumin was also considered. In this case, it can be predicted (theoretical model not shown) that the rate constant of the fast phase should decrease or, at most, should remain constant with a decreasing concentration of vesicles. As an important increase is observed (Figure 7), this mechanism cannot be a preponderant process. It can be noted also that the rate constant of the fast phase reaches a plateau at high albumin concentrations, which is another proof that the transfer is a diffusive rather than a collisional process.

The effect of albumin and vesicle concentration on the slow-phase rate constant was, by far, less important than that on the fast phase. The constants at 32 °C ranged between 0.4 and 0.8 s^{-1} for all the extruded vesicles studied, and the amplitude of changes hardly exceeds the experimental errors (see Figure 7). It was, however, possible according to eq 14 to have estimates of k_{to} from the average values obtained for high albumin concentrations. The values of k_{to} along with those of $k_{ti} + k_{to}$, the latter being obtained in the experiments carried out without albumin, are given in Table 1. Except for the sonicated vesicles, no significant size effect is seen. The values of k_{ti} and k_{to} being known, the equilibrium constant K_L can be derived from eq 6. These calculated values (noted K_L^{kin}) agree quite well with the equilibrium constants (noted K_L^{eq}) obtained by steady-state measurements (see Table 1), except for the sonicated vesicles. It can be noted that no significant difference between k_{to} and k_{ti} was observed. This was quite unexpected in the case of sonicated vesicles, which have inequivalent volumes of lipids in the outer half as compared to the inner half of the bilayer. These discrepancies might be due to additional effects of geometric constraints (Huang & Mason, 1978).

The validity of Schemes 1 and 2 is fully supported by all the kinetic and steady-state measurements. Moreover, from the kinetic constants determined above, the rate constants for

the reverse transfer of the porphyrin (from albumin to vesicles) can be predicted using eq 10. Thus, for [DMPC] = 2×10^{-3} M and [HSA] = 5.7×10^{-6} M, k_1 and k_2 can be calculated to be 5.5 and 0.62 s^{-1}, respectively, in excellent agreement with the measured values (see Results). Other hypotheses on the nature of the slow phase, such as self-association of the porphyrin at the phospholipid–water interface, can be disregarded in view of the above remarks of the fluorescence changes observed and because the phospholipid concentration largely exceeds that of the porphyrin.

The observed effects of temperature and cholesterol further support Scheme 2. In the experiments described in Figure 8a, the rate of the fast phase is dominated, for the highest albumin concentration, by the interactions of the porphyrin with the phospholipid bilayer (especially by the value of k_{off}, see eq 13). The break of the plot at the phase transition temperature is characteristic for transfer processes from lipidic vesicles. For the lowest albumin concentration, the fast phase is predicted to be governed by k_{dis} rather than by rate constants involving the vesicles (see eq 11 and Figure 7). In this case, the plot reflects mainly the influence of temperature on the dissociation from albumin. In keeping with the negligible effect of temperature on the affinity of DP for albumin (Rotenberg et al., 1987), the evolution seen in Figure 8 is moderate with no break in the plot.

In the case of DMPC–cholesterol vesicles, only a moderate effect of temperature on the kinetics was observed, and the signal remained monoexponential. The rate constant smoothly varies, even around 23 °C (see Figure 8c). In comparison with pure DMPC vesicles, the transfer to albumin is more rapid below 23 °C and slower at higher temperatures. This behavior is explained by the well-known effect of cholesterol that smooths off the phase transition of phospholipid bilayers (Papahadjopoulos et al., 1973). The exit rate of the porphyrin from the vesicles is thus closely coupled to the degree of packing of the bilayer. Similarly, cholesterol was shown to slow down the dissociation of hemin from phosphatidylcholine–dicetylphosphate or phosphatidylcholine–stearylamine vesicles at room temperature (Cannon et al., 1984).

The drastic effect of the temperature on the slow phase is also fully consistent with the view that this phase is essentially controlled by the transfer of the porphyrin between the monolayers. A marked increase of the rate is found when the vesicles are in the fluid state. Moreover, at the temperature of phase transition, a sharp enhancement of the rate is seen. Similar effects on the transport across DMPC vesicles were previously observed for a number of other species: e.g., anilinonaphthalene sulfonate (Tsong, 1975) and heme (Light & Olson, 1990). As suggested by Papahadjopoulos et al. (1973), this behavior is likely due to increased transfer at boundaries between liquid and solid domains, which are formed in the bilayer during the phase transition.

In the case of DMPC–cholesterol vesicles, movement through the bilayer is probably too slow (k_{ti}, $k_{to} < 0.05$ s^{-1}) to be observed in stopped-flow experiments. Similarly, as reported by Tsong (1975), the fluorescence signal corresponding to the transport of anilinonaphthalene sulfonate across a DMPC–cholesterol bilayer completely disappears from the 33% mole fraction of cholesterol. On the other hand, the flip-flop movement of deuteroporphyrin might be too fast and overlap with the first phase in the case of egg phosphatidylcholine vesicles for which only a monoexponential signal was observed at 22 °C (Vever-Bizet & Brault, 1993). Significantly greater transfer rates in egg phosphatidylcholine vesicles as compared to DMPC vesicles were observed recently in the case of long-chain fatty acids (Kleinfeld & Storch, 1993).

Some common features are presented by deuteroporphyrin and other hydrophobic amphiphiles. The initial interaction of these molecules with vesicles is a diffusion-controlled process as shown by (i) the order of magnitude of the rate constant which is comparable to that predicted by eq 18 [see also Vever-Bizet and Brault (1993)], (ii) its dependence on vesicle size outlined here, and (iii) medium viscosity effects (Woolley & Diebler, 1979). The exit rate is controlled both by properties of the lipidic bilayer, namely, its fluidity, and by properties of the solubilized molecule. The hydrophobicity (Almgren, 1980; Pownall et al., 1983; Vever-Bizet & Brault, 1993) and the charge of the molecule, which can be modulated by pH (Doody et al., 1980; Vever-Bizet & Brault, 1993), are the main determinants of the exit rate. Values obtained with deuteroporphyrin are comparable to those found with perylene (3.4 s^{-1}) and pyrene (50 s^{-1}) as reported by Almgren (1980) or with bilirubin (Zucker et al., 1992). Molecules with an asymmetric arrangement of polar chains (or charges) distribute, and may undergo exchange, between leaflets. This process appears to be extremely sensitive to the state of the bilayer. The structural features of the solubilized molecules governing this exchange remain to be elucidated in detail.

In the case of carboxylic porphyrins, the exit process and the movement across the bilayer are fast enough to postulate that redistribution within various compartments in cells occurs quickly. Even if a lipoprotein-mediated uptake mechanism is preponderant, which would drive the porphyrin to endosomes and lysosomes, it is likely that the porphyrin will leak out these subcellular structures in favor of other compartments such as mitochondria (Salet & Moreno, 1990). These processes must also be taken into account in drug delivery using liposomes. The exchange of photosensitizers between liposomes and serum proteins is expected to be fast, even in the case of hydrophobic compounds. Such a redistribution has been noted in the case of DMPC vesicles (Ginevra et al., 1990). All these examples emphasize the importance of considering mechanisms from a kinetic point of view. The transfer of molecules from vesicles to albumin, which has been analyzed in detail in the present study, presents several advantages over the system involving only vesicles. The uncertainty in the k_{off} value is much reduced. Moreover, it makes it possible to study hydrophobic molecules insoluble in water and allows for discrimination between the two directions of transfer through the bilayer.

ACKNOWLEDGMENT

We are grateful to Dr. P. Kuzel for his help in data analysis and to Pr. P. Couvreur and Dr. E. Fattal for measurements of vesicle sizes. Thanks are due to Dr. P. King for his guidance in the preparation of the manuscript. We are indebted to Dr. C. Vever-Bizet for her contribution in the initial development of this work.

APPENDIX

Interaction of Porphyrin with Vesicles. The solution of the system (eq 1) of kinetic equations can be easily found by using the Laplace transform (Rodiguin & Rodiguina, 1964). With the initial conditions $P_f(t = 0) = P_f^0$ and $P_o(t = 0) = P_i(t = 0) = 0$, the system is transformed to

$$\omega P_f - P_f^0 = -k_{on}' P_f + k_{off} P_o$$

$$\omega P_o = k_{on}' P_f - (k_{off} + k_{ti}) P_o + k_{to} P_i$$

$$\omega P_i = k_{ti}P_o - k_{to}P_i$$

and yields

$$P_f = \frac{P_f^0(\omega^2 + \omega(k_{off} + k_{ti} + k_{to}) + k_{off}k_{to})}{\omega D}$$

$$P_o = \frac{k_{on}'P_f^0(\omega + k_{to})}{\omega D}$$

$$P_i = \frac{k_{on}'k_{ti}P_f^0}{\omega D}$$

where $D = \omega^2 + \omega(k_{on}' + k_{off} + k_{ti} + k_{to}) + k_{on}'k_{ti} + k_{off}k_{to} + k_{on}'k_{to}$.

The inverse Laplace transform gives the expressions describing the evolution of P_f, P_o, and P_i as a function of time. The expressions consist of one constant and two exponential terms. The rate constants k_1 and k_2 are found by converting D into the form $(\omega + k_1)(\omega + k_2)$, i.e., by finding the roots (k_1, k_2, abbreviated $k_{1,2}$) of the equation $D = 0$:

$$k_{1,2} = \frac{1}{2}(\sum k \pm [(\sum k)^2 - 4(k_{on}'k_{ti} + k_{off}k_{to} + k_{on}'k_{to})]^{1/2})$$

where $\sum k = k_{on}' + k_{off} + k_{ti} + k_{to}$.

If $4(k_{on}'k_{ti} + k_{off}k_{to} + k_{on}'k_{to})$ is small compared to $(\sum k)^2$ (in our case <6% as indicated by the experimental results), the square root can be expanded as a Taylor series and one can write

$$k_{1,2} \cong \frac{\sum k}{2}\left[1 \pm \left(1 - \frac{2(k_{on}'k_{ti} + k_{off}k_{to} + k_{on}'k_{to})}{(\sum k)^2}\right)\right]$$

Substituting k_{on}' by k_{on}[DMPC] and neglecting small terms (errors resulting from the approximation are evaluated in the discussion) give

$$k_1 \cong k_{on}[\text{DMPC}] + k_{off} + k_{ti} + k_{to}$$

$$k_2 \cong k_{ti} + k_{to}$$

Transfer of Porphyrin from Vesicles to Albumin. Using the steady-state approximation of Bodenstein (Benson, 1960), we transform eq 8 to a more simple one (eq 9), which is practically identical with that described above. With initial conditions of $P_i(t = 0) = P_i^0$, $P_o(t = 0) = P_o^0$, and $P_b(t = 0) = 0$, the expressions for P_i, P_o, and P_b in the Laplace space are

$$P_i = \frac{P_o^0(\omega + \delta)\beta + P_i^0(\omega^2 + \omega(\delta + \beta + \gamma) + \beta\delta)}{\omega D}$$

$$P_o = \frac{P_o^0(\omega + \delta)(\omega + \alpha) + P_i^0\alpha(\omega + \delta)}{\omega D}$$

$$P_b = \frac{P_o^0\gamma(\omega + \alpha) + P_i^0\alpha\gamma}{\omega D}$$

where $D = \omega^2 + \omega(\alpha + \beta + \gamma + \delta) + \alpha\gamma + \alpha\delta + \beta\delta$.

As in the preceding paragraph, the evolution of P_i, P_o, and P_b versus time is described by one constant and two exponential terms which are found by the inverse Laplace transform. The rate constants are the roots of the equation $D = 0$.

REFERENCES

Almgren, M. (1980) *J. Am. Chem. Soc. 102*, 7882–7887.

Atkins, P. W. (1990) *Physical Chemistry*, Oxford University Press, Oxford.

Bartlett, G. R. (1959) *J. Biol. Chem. 234*, 466–468.

Benson, S. W. (1960) *The foundation of chemical kinetics*, McGraw-Hill Book Co., New York.

Berg, K., Western, A., Bommer, J. C., & Moan, J. (1990) *Photochem. Photobiol. 52*, 481–487.

Blum, A., & Grossweiner, L. I. (1985) *Photochem. Photobiol. 41*, 27–32.

Blume, A. (1979) *Biophys. Chem. 10*, 371–378.

Brault, D. (1990) *J. Photochem. Photobiol. B 6*, 79–86.

Brault, D., Vever-Bizet, C., & Le Doan, T. (1986) *Biochim. Biophys. Acta 857*, 238–250.

Cannon, J. B., Kuo, F.-S., Pasternack, R. F., Wong, N. M., & Muller-Eberhard, U. (1984) *Biochemistry 23*, 3715–3721.

Clarke, R. J., & Apell, H.-J. (1989) *Biophys. Chem. 34*, 225–237.

Daniels, C., Noy, N., & Zakim, D. (1985) *Biochemistry 24*, 3286–3292.

Dellinger, M., & Brault, D. (1987) *J. Chromatogr. 422*, 73–84.

De Smidt, P. C., Versluis, A. J., & Van Berkel, Th. J. C. (1993) *Biochemistry 32*, 2916–2922.

Doody, M. C., Pownall, H. J., Kao, Y. J., & Smith, L. C. (1980) *Biochemistry 19*, 108–116.

Dougherty, T. J., Potter, W. R., & Bellnier, D. (1990) in *Photodynamic Therapy of Neoplastic Disease* (Kessel, D., Ed.) Vol. I, pp 1–19, CRC Press, Boston.

Ginevra, F., Biffanti, S., Pagnan, A., Biolo, R., Reddi, E., & Jori, G. (1990) *Cancer Lett. 49*, 59–65.

Henderson, B. W., & Dougherty, T. J. (1992) *Photochem. Photobiol. 55*, 145–157.

Huang, C.-H. (1969) *Biochemistry 8*, 344–352.

Huang, C.-H., & Mason, J. T. (1978) *Proc. Natl. Acad. Sci. U.S.A. 75*, 308–310.

Jori, G., Beltramini, M., Reddi, E., Salvato, B., Pagnan, A., Ziron, L., Tomio, L., & Tsanov, T. (1984) *Cancer Lett. 24*, 291–297.

Kleinfeld, A. M., & Storch, J. (1993) *Biochemistry 32*, 2053–2061.

Kongshaug, M., Moan, J., & Brown, S. B. (1989) *Br. J. Cancer 59*, 184–188.

Light, W. R., & Olson, J. S. (1990) *J. Biol. Chem. 265*, 15623–15631.

Margalit, R., & Rotenberg, M. (1984) *Biochem. J. 219*, 445–450.

Mayer, L. D., Hope, M. J., & Cullis, P. R. (1986) *Biochim. Biophys. Acta 858*, 161–168.

Moan, J., & Berg, K. (1991) *Photochem. Photobiol. 53*, 549–553.

Moan, J., & Berg, K. (1992) *Photochem. Photobiol. 55*, 931–948.

Moan, J., Smedshammer, L., & Christensen, T. (1980) *Cancer Lett. 9*, 327–332.

Nayar, R., Hope, M. J., & Cullis, P. R. (1989) *Biochim. Biophys. Acta 986*, 200–206.

Oenbrink, G., Jürgenlimke, P., & Gabel, D. (1988) *Photochem. Photobiol. 48*, 451–456.

Olson, F., Hunt, C. A., Szoka, F. C., Vail, W. J., & Papahadjopoulos, D. (1979) *Biochim. Biophys. Acta 557*, 9–23.

Papahadjopoulos, D., Jacobson, K., Nir, S., & Isac, T. (1973) *Biochim. Biophys. Acta 311*, 330–348.

Peng, Q., Moan, J., & Cheng, L.-S. (1991) *Cancer Lett. 58*, 29–35.

Pownall, H. J., Hickson, D. L., & Smith, L. C. (1983) *J. Am. Chem. Soc. 105*, 2440–2445.

Press, W. H., Flannery, B. P., Teukolsky, S. A., & Vetterling, W. T. (1988) in *Numerical Recipes: The Art of Scientific Computing*, Chapter 14, Cambridge University Press, New York.

Rakowski, A. (1906) *Z. Phys. Chem. 57*, 321–340.

Reyftmann, J. P., Morliere, P., Goldstein, S., Santus, R., Dubertret, L., & Lagrange, D. (1984) *Photochem. Photobiol. 40*, 721–729.

Ricchelli, F., Jori, G., Gobbo, S., & Tronchin, M. (1991) *Biochim. Biophys. Acta 1065*, 42–48.

Rodiguin, N. M., & Rodiguina, E. N. (1964) *Consecutive chemical reactions*, D. Van Nostrand Co., Princeton, NJ.

Rotenberg, M., Cohen, S., & Margalit, R. (1987) *Photochem. Photobiol. 46*, 689–693.

Salet, C., & Moreno, G. (1990) *J. Photochem. Photobiol. B 4*, 133–150.

Shulock, J. R., Wade, M. H., & Lin, C.-W. (1990) *Photochem. Photobiol. 51*, 451–457.

Spikes, J. D., & Straight, R. C. (1990) in *Photodynamic Therapy of Neoplastic Disease* (Kessel, D., Ed.) Vol. I, pp 211–228, CRC Press, Boston.

Storch, J., & Kleinfeld, A. M. (1986) *Biochemistry 25*, 1717–1726.

Thomas, J. P., & Girotti, A. W. (1989) *Photochem. Photobiol. 49*, 241–247.

Tsong, T. Y. (1975) *Biochemistry 14*, 5409–5414.

Vever-Bizet, C., & Brault, D. (1993) *Biochim. Biophys. Acta 1153*, 170–174.

Watts, A., Marsh, D., & Knowles, P. F. (1978) *Biochemistry 17*, 1792–1801.

Woolley, P., & Diebler, H. (1979) *Biophys. Chem. 10*, 305–318.

Zana, R. (1986) in *Surfactants in Solution* (Mittal, K., & Bothorel, P., Eds.) pp 115–130, Plenum Press, New York.

Zucker, S. D., Storch, J., Zeidel, M. L., & Gollan, J. L. (1992) *Biochemistry 31*, 3184–3192.